Analytical Model for Liquid Rocket Propellant Feedline Dynamics

JESSE L. HOLSTER* AND WILLIAM J. ASTLEFORD†
Southwest Research Institute, San Antonio, Texas

A generalized analytical model and computer program have been developed to predict the frequency response of arbitrary liquid propellant feedline designs. The analytical model is based on an extension of an existing distributed parameter representation of a viscous fluid transmission line with laminar flow which was modified to include the effects of a turbulent mean flow. The effects of dissolved ullage gases, wall elasticity, localized gas or vapor bubbles, bellows, forced changes in length due to structural excitation, complex side branches, and structural mounting stiffness are also included. Each line component is written as a four-terminal, pressure-flow relationship in matrix form in the Laplace domain; the transfer function relating the pressure response at the line terminal (inducer inlet) to the external excitation is obtained in the computer program by sequential matrix substitution.

Nomenclature

A = cross sectional area
a = acceleration
$\mathbf{B}, \mathbf{D}, \mathbf{P}, \mathbf{Q}$ = matrices of the final transfer function
b = damping coefficient
b_{ij}, d_{ij} = elements of matrices **B** and **D**
C = compliance
$\mathbf{C}_i$ = matrix representing the effect of an external forcing function
c = phase velocity
c_o, c_g, c_l, c_w = speed of sound in the fluid mixture, gas, liquid, and wall, respectively
D = thermal diffusivity
E = elastic modulus
F = external forcing parameter
f = bellows friction factor
$G(s)$ = transfer function relating two structural velocities
h = wall thickness
I = line inertance, $\rho_o L/A$
i = imaginary number, $(-1)^{1/2}$
J_o, J_1 = Bessel functions of the first kind
K = spring constant
k_b = bellows volume change constant
k = ratio of specific heats
L = line segment length
M, m = mass
m_e = effective mass
N_R = Reynolds number
$P(s)$ = Laplace transform of pressure perturbation, $p(t)$
P_o = mean bubble or gas volume pressure
p_o, p, p_t = mean pressure, dynamic and turbulent pressure perturbation
$Q(s)$ = Laplace transform of volume flow perturbation
$q(t)$ = volume flow perturbations
R = line resistance
R_o = mean bubble radius
r = radial displacement
r_o = line or branch radius
$S; \Delta S_{gl}$ = entropy; change in entropy between saturated vapor and liquid state
s = Laplace variable
T = temperature
t = time
$U_w(s)$ = Laplace transform of $\dot{x}(t)$
u_o, u, u_t = mean axial velocity, dynamic and turbulent perturbation
$\bar{V}$ = total velocity vector
$V(s)$ = Laplace transform of $v(t)$
V_o = mean bubble volume
v_g, v_l = specific volume of the gas and liquid
v_r = radial velocity component
$X(s)$ = Laplace transform of $x(t)$
x = axial displacement
Z_c, Z_i, Z_t = line characteristic impedance, inlet impedance and terminal impedance
α = attenuation factor
γ = propagation operator
δ = logarithmic decrement/π
ζ = $2J_1(\xi r_o)/\xi r_o J_o(\xi r_o)$
η = polytropic exponent
θ = $0.011\nu(N_R)^{0.85}/r_o^2$
κ = liquid bulk modulus
μ = viscosity
ν = kinematic viscosity
ξ = $(-s/\nu)^{1/2}$
ρ_o, ρ_g, ρ_l = density of mixture, density of gas, and density of liquid
υ = volume perturbations
Φ = mass of gas/mass of liquid
ϕ = $(\omega/2D)^{1/2}$
χ = mixture quality, mass vapor/total mass
ψ = phase angle
ω = angular frequency
∇ = differential operator

Introduction

AT least three classes of propulsion feed system instabilities have been identified in liquid propellant rockets.[1-6] In each case, the dynamic behavior of the feedline played a major role in the instability. Probably the best known problem involves a closed-loop coupling of the vehicle longitudinal structural modes, the feed system, and the engine.[1-2] The name POGO has been assigned to this class of vibration instability, and its theory has been very well described by Rubin.[3] On Saturn flight AS-504 the S-II center engine displayed severe pressure and thrust oscillations rather late in the stage burn.[4] In this case, the problem was localized and involved a closed-loop instability of the engine support structure, the feed system and the engine. A second type of problem which can exist involves only the feed system, the inducer-pump combination, and the engine.[5] This instability can be traced directly to the inducer dynamics, with the feed system and engine providing an impedance loading which governs the resultant oscillation frequency. Reference 6 notes a third type of instability involving feedsystem and combustion chamber interaction sometimes referred to as "chugging" or "buzzing."

Received March 23, 1973; revision received July 30, 1973. This research was supported by the George C. Marshall Space Flight Center under Contract NAS8-25919.

Index categories: LV/M Dynamics, Uncontrolled; Liquid Rocket Engines; Wave Motion and Sloshing.

* Research Engineer, Department of Mechanical Sciences. Member AIAA.

† Senior Research Engineer, Department of Mechanical Sciences.

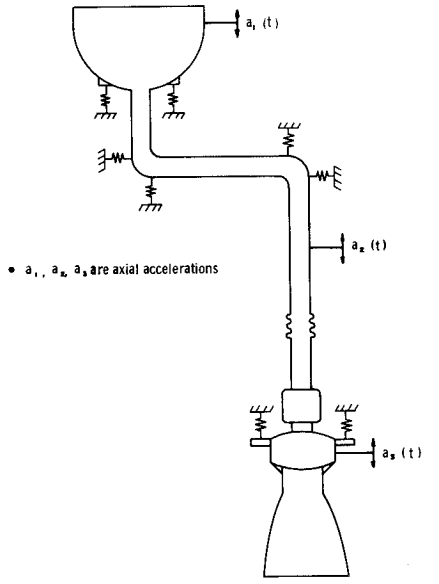

Fig. 1 Hypothetical feed system and engine.

All of the previous instabilities pose a threat to the success of a mission. For simulation purposes, it is readily recognized that adequate modeling procedures are needed for each portion of the vehicle involved in a given instability. A computer program, based on an analytical model, has been developed which facilitates studies on the effect of disturbances in the liquid propellants of typical feedline systems. The problem of modeling a given feedline is illustrated in Fig. 1, where a hypothetical system involving a propellant tank, a feedline, a pump, and an engine is given. In general, each element of the model is elastically supported and can experience motion relative to a body-fixed frame of reference on the vehicle. These accelerations, plus pressure oscillations in the engine combustion chamber and cavitating inducer instabilities, represent disturbance inputs to the feed system which can cause flow and pressure oscillations. These disturbances may, in turn, couple back with the engine and/or structure to produce a large amplitude, closed-loop instability. The modeling problem, with respect to the feed system, is to describe analytically the perturbation pressure and flow at the pump inlet or line terminal in response to the application of proper end conditions, acceleration inputs, and structural supports.

General Line Model

Modeling liquid propellant feedline dynamics is, in itself, not new. In fact, many models have been developed in the past. In general, these models were developed for a specific configuration or launch vehicle; those that are more general do not adequately treat all the effects which are considered here.

To exactly describe the dynamic fluid behavior in a feedline segment would require simultaneous solution of an equation of motion given in vector form by

$$(\partial \bar{V}/\partial t)+(\bar{V}\cdot\nabla)\bar{V}=(-\nabla p/\rho)+\nu[\tfrac{4}{3}\nabla(\nabla\cdot\bar{V})-\nabla\times(\nabla\times\bar{V})] \quad (1)$$

plus a continuity equation

$$\partial\rho/\partial t+\nabla\cdot(\rho\bar{V})=0 \quad (2)$$

and a fluid equation of state valid for a liquid

$$dp=\kappa(d\rho/\rho) \quad (3)$$

The above nonlinear formulation is extremely complex, and all feedline models developed to date, including that described herein, represent the solution of some reduced form of this set of equations. In most of the early models, the viscous effects were completely neglected. Perhaps the earliest work dates back to Sabersky,[7] who used an inviscid line model to analyze the low frequency combustion instability of a liquid rocket. Woods[8] applied the method of characteristics to a frictionless model to study the flow perturbations in feedlines. A more general nonlinear distributed parameter model for calculating unsteady flow in liquid filled rocket propellant feed systems was developed at the NASA Lewis Research Center, which the authors called the wave-plan method.[9] A generalized digital computer program was also developed and the line viscous effects were treated by imaginary orifices distributed along the line length.[10] Fashbaugh and Streeter[11] also employed a very reduced form of the equations of motion, given by

$$\partial u/\partial t=-(1/\rho_o)(\partial p/\partial x)-Ru^2 \quad (4)$$

with the term Ru^2 replacing the viscous dissipation terms to approximate turbulence losses. While these two models have the advantage of treating nonlinear effects and the transient response, they improperly represent friction as a function of frequency. Zielke et al.[12] used a one-dimensional compressible fluid approach with a linearized resistance proportional to the perturbation velocity; that is, Ru replaced the term Ru^2 in Eq. (4). These authors presented a standard "operator form" solution of the describing equations which provides a convenient means of evaluating frequency response and transfer functions for periodic motion. Rose[13] also used a similar technique to model the feedline in his stability analysis of liquid rockets. Wing and Tai[14] presented a linear "operator" model which gives a frequency description of a line with a compressible fluid including an effect of the mean flow and linearized friction. None of these models properly represent friction as a function of frequency, especially when the flow is turbulent. Only the models described in Refs. 10 and 13 are applicable to arbitrary feedline systems, and these models do not treat all the factors which affect feedline dynamics that are considered herein.

Generally, a feedline may be regarded as a series of elements, such as lengths of line, local compliances, branches, bellows, etc. Therefore, it is necessary to describe each element individually, and then define means for mathematically combining these elements so as to produce the proper over-all system model. In this paper, each element is basically defined by a four-terminal representation in the Laplace domain; over-all system model formulation is also achieved in the Laplace domain. In this manner, the frequency response of the feedline system excited by oscillatory perturbations can be obtained by substitution of $i\omega$ for the Laplace variable, s. The phase angle relating the terminal pressure to the excitation input is also computed so that a complete Bode plot can be constructed.

Expanding the momentum Eq. (1) in cylindrical coordinates and assuming axisymmetric flow with $\bar{u}\gg\bar{v}_r$, the momentum equation becomes

$$\frac{\partial\bar{u}}{\partial t}+\bar{u}\frac{\partial\bar{u}}{\partial x}+\bar{v}_r\frac{\partial\bar{u}}{\partial r}=\frac{-\partial p}{\rho\partial x}+\nu\left[\frac{4}{3}\frac{\partial^2\bar{u}}{\partial x^2}+\frac{\partial^2\bar{u}}{\partial r^2}+\frac{1}{r}\frac{\partial\bar{u}}{\partial r}+\frac{1}{3}\frac{\partial}{\partial x}\left(\frac{\partial\bar{v}_r}{\partial r}+\frac{\bar{v}_r}{r}\right)\right] \quad (5)$$

Likewise, the continuity equation is

$$\frac{\partial\rho}{\partial t}+\rho\frac{\partial\bar{v}_r}{\partial r}+\rho\frac{\bar{v}_r}{r}+\rho\frac{\partial\bar{u}}{\partial x}+\bar{v}_r\frac{\partial\rho}{\partial r}+\bar{u}\frac{\partial\rho}{\partial x}=0 \quad (6)$$

The vector velocity and pressure at any point in the line may be assumed to consist of a sum of three components: 1) a mean time invariant term, 2) a time dependent term denoting the dynamic behavior of interest, and 3) a time dependent part representing the turbulent fluctuations in the line. Close examination of Eqs. (5) and (6) by substitution of the assumed velocity components given in Fig. 2 has shown that the presence of a mean turbulent flow has two possible effects. First, the turbulent terms introduce dissipation over and above the conventional laminar damping. Second, the mean flow, u_o, introduces a "convective" effect. The linearization of Eqs. (5) and (6) by neglecting these convective terms can be justified since they are small when compared with the other terms; this is shown in detail by D'Souza and Oldenburger.[15] The solution of the resulting differential equations accounts for laminar viscous

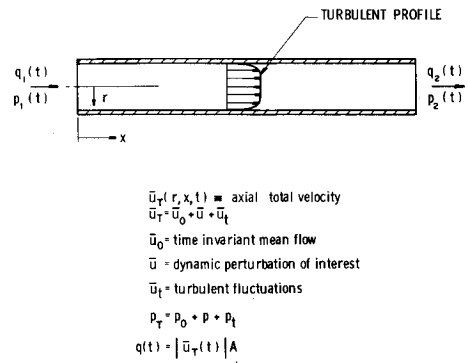

Fig. 2 General physical picture of flow behavior in feed line.

effects, but does not apply to flow with turbulence. The requirements for a dynamic feedline model with turbulent flow are that the attenuation or viscous effects of the turbulent flow be properly treated. The turbulent flow model presented in this paper is an extension of an existing distributed parameter model.[15-17]

Following the further linearization of Eqs. (1-3) as outlined in Ref. 15, the following two differential equations are obtained

$$\rho\frac{\partial u}{\partial t} = \frac{-\partial p}{\partial x} + \mu\left[\frac{\partial^2 u}{\partial r^2} + \frac{1}{r}\frac{\partial u}{\partial r}\right] \tag{7a}$$

$$\frac{1}{\kappa}\frac{\partial p}{\partial t} + \frac{\partial v_r}{\partial r} + \frac{v_r}{r} + \frac{\partial u}{\partial x} = 0 \tag{7b}$$

The solution of these equations in the Laplace domain may be written as

$$\begin{aligned} P_2(s) &= P_1(s)\cosh(\gamma L) - Z_c A^{-1} Q_1(s)\sinh(\gamma L) \\ Q_2(s) &= Q_1(s)\cosh(\gamma L) - Z_c^{-1} A P_1(s)\sinh(\gamma L) \end{aligned} \tag{8}$$

Here, $P(s)$ and $Q(s)$ represent the transformed pressure and volume flow perturbations, respectively, at two points along the line separated by a distance, L. The laminar propagation operator takes the familiar form

$$\gamma_{\text{lam}} = \frac{s}{c}\left[1 - \frac{2J_1(\xi r_o)}{\xi r_o J_o(\xi r_o)}\right]^{-1/2} \tag{9}$$

The characteristic impedance is related to the propagation operator by

$$Z_c = \rho_o c_o^2 \gamma / s \tag{10}$$

The physical interpretation of the propagation operator and the characteristic impedance can be best illustrated by considering a semi-infinite line. For this special case, the pressure perturbation at a downstream location, x_2, is related to the upstream pressure perturbation at x_1 by

$$P(x_2, s) = P(x_1, s)\, e^{-[\gamma(s)(x_2 - x_1)]} \tag{11}$$

and the pressure at a particular cross section is related to the flow at that cross section by

$$\frac{P(x, s)}{Q(x, s)} = Z_c(s) \tag{12}$$

The attenuation factor, α, is determined by evaluating the real part of the propagation operator,

$$\alpha = \text{Real}\,[\gamma(s)] = \gamma_r \tag{13}$$

Effect of Turbulence

It is known that the four-terminal Laplace domain representation for pressure and flow in a line is extremely accurate when the flow is laminar and the propagation operator is as given by Eq. (9). In reality, a turbulent flow condition exists for many propellant feedline operating points, as indicated by Reynolds numbers of the order of 10^5 to 5×10^7. The effect of turbulence must be reflected in the propagation operator, since in Fig. 3 (from Ref. 18) it is observed that for a given line size, fluid, and frequency, the attenuation is increased at some frequencies by as much as a factor of 100 over that predicted by the laminar model. At high frequencies, the laminar and turbulent attenuations coincide. There is also some tendency for turbulence to reduce the phase velocity at very low frequencies and high Reynolds numbers.[18] However, after a thorough investigation into existing feedline geometries, propellant properties, mean flow velocities, and the frequency range for structural-hydraulic coupling, we have concluded that the effect of turbulence on the phase velocity can be neglected.

For the distributed parameter line model, the effect of turbulent attenuation has been modeled by adding to the existing laminar attentuation factor, γ_r, an additional attenuation contribution, γ_t, due to turbulence.

$$\alpha = \gamma_r + \gamma_t \tag{14}$$

Thus, a new propagation operator, γ, has been created to account for the effect of the turbulent mean flow.

$$\gamma = (\gamma_r + \gamma_t) + i\gamma_i \tag{15}$$

The form of the turbulence-induced increment in attenuation

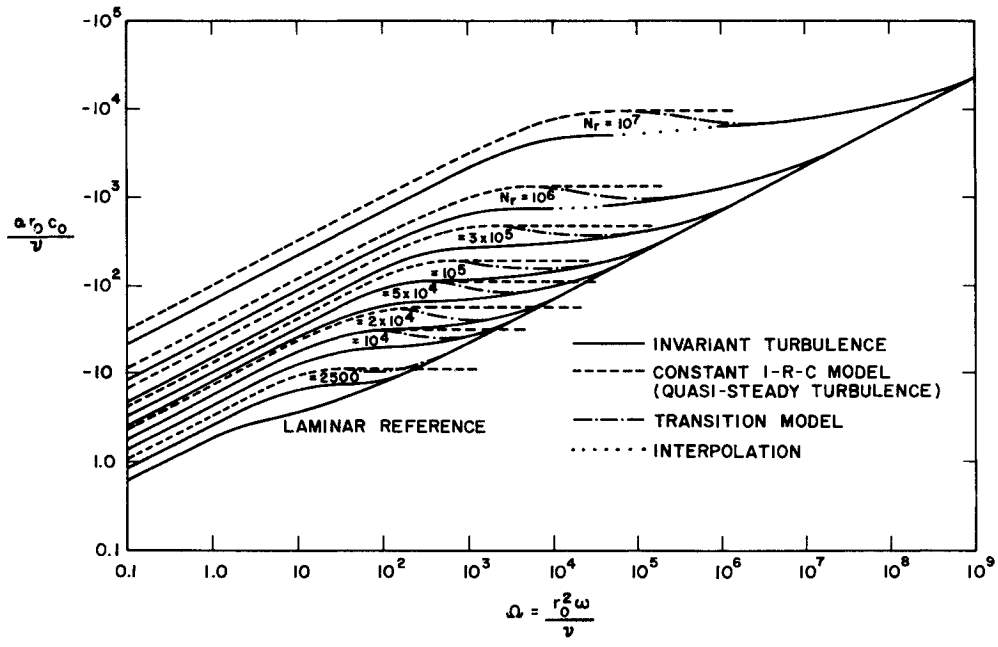

Fig. 3 Predictions of attenuation factor for turbulent flow.[18]

was derived from the form of the attenuation factor of a constant *I-R-C*, lumped parameter, representation of a line. That is,

$$\gamma_{IRC} = Re\{s(CI)^{1/2}(R/Is+1)^{1/2}\} \tag{16}$$

where *Re* denotes the real part of the quantity in the brackets. By analogy

$$\gamma_t = \text{Real}\,[(s/c_o)(\theta/s+1)^{1/2}] \tag{17a}$$

where

$$\theta = \frac{0.011\nu N_R{}^{0.85}}{r_o{}^2} \tag{17b}$$

The constants in Eq. (17b) were determined by surface fitting the difference in the invariant turbulent attenuation and the laminar reference given in Fig. 3 as a function of Reynolds number and frequency.

Entrained Gases

In most practical applications, the liquid rocket propellant in the feedline contains quantities of either dissolved ullage gas or propellant vapor, or possibly both. For modeling purposes, it is assumed that the gases or vapor are in the form of small bubbles, homogeneously distributed throughout the liquid. It is important to include the effect of entrained gas since the net effect of distributed bubbles in the liquid is to modify (reduce) the effective fluid sonic velocity and possibly to introduce added damping because of irreversible compression and expansion of the bubbles caused by a periodic disturbance. This change in sonic velocity can significantly alter the line response with only small amounts of dissolved gases present.

Two types of entrained gases have been considered in the model for the acoustic velocity in a two-phase flow: 1) the flow of a single-component, two-phase mixture, such as LOX and oxygen vapor, and 2) the flow of a two-component, two-phase mixture, such as LOX with entrained helium ullage gas.

For a single-component, two-phase mixture, the actual flow process is theoretically bounded by the equilibrium process and the constant quality process. In the case of an equilibrium process, the vaporization and condensation rates are large enough to ensure that the vapor temperature and the liquid temperature are always equal; both phases are saturated, and the quality (vapor fraction by weight) varies only with pressure. Based on the assumption of thermodynamic equilibrium, Gouse and Brown[19] have shown that the speed of sound in a single-component, two-phase flow can be expressed as

$$c_o = \left(\frac{v_l}{v_g - v_l} + \chi\right)\Delta S_{gl}\left[g_o\left(\frac{\Delta T}{\Delta S}\right)_v\right]^{1/2} \tag{18}$$

Evaluation of Eq. (18) requires the extensive use of a temperature-entropy chart or a tabular representation of the thermodynamic properties of the fluid being considered.

On the other hand, the condensation and vaporization rates in a constant quality process are assumed to be so low that no significant phase change occurs. In a two-component mixture, a constant quality exists at all times if there is no liquid vapor present. Rearranging the derivation by Hsieh and Plesset,[20] the speed of sound in a two-component mixture is

$$\frac{1}{c_o{}^2} = \rho\left[\left(\frac{\rho_g}{\rho_g+\Phi\rho_l}\right)\frac{1}{\rho_l}\frac{1}{c_l{}^2} + \left(\frac{\Phi\rho_l}{\rho_g+\Phi\rho_l}\right)\frac{1}{\rho_g}\frac{1}{c_g{}^2}\right] \tag{19}$$

As the mass ratio, Φ, approaches zero, the speed of sound approaches that for the pure liquid. Plesset and Hsieh[21] have also shown that, for very small gas bubbles dissolved in a liquid, the adiabatic speed of sound in the gas should be replaced by the isothermal speed of sound. The reason is that the gas bubbles have a nonuniform temperature distribution in their interior due to the finite value of the heat conduction rate. Figure 4 presents the isothermal vs the adiabatic model for dissolved helium ullage gas in LOX. For comparison, the equilibrium model for LOX with O_2 vapor is also shown. Reliable experimental data are not available to determine which flow process

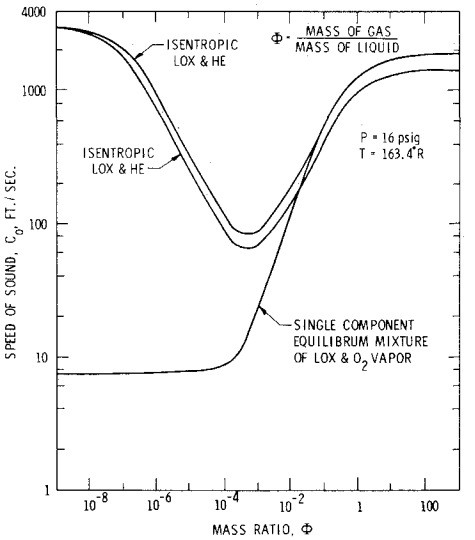

Fig. 4 Variation of speed of sound with mass ratio.

actually occurs for the flow of a single-component, two-phase mixture. As can be seen by Fig. 4, there is a great difference in the acoustic velocity between the equilibrium and the constant quality flow processes. These differences could lead to a large error in the predicted feedline system response, and more work should be devoted to a study of the actual flow process. In the present study, the constant quality model is applied to both single-component and two-component flows.

Wall Elasticity

The flexibility of the feedline wall will produce two possible effects which may be of concern. Firstly, the wall compliance will reduce the phase velocity and increase the spatial attenuation for the longitudinal fluid wave propagation mode (called the zeroeth mode in Ref. 22), and secondly, the axial wall stiffness could permit real wave propagation of the higher order modes at low frequency by virtue of coupling between the fluid and axial wall modes. For typical feedline problems, the amount of energy which is fed into the higher order modes at the line terminations is so small that it can be neglected; thus, the effect of the axial wall stiffness can be neglected. Gerlach[22] has shown that the radial attenuation for an elastic wall is virtually indistinguishable from the attenuation of a rigid wall over the frequency range encountered in practical feedline problems. Therefore, only a correction to the phase velocity is required, and, for thin-walled feedlines, the classic Korteweg correction is valid.

$$c = \frac{c_o}{[1+(2\rho_o c_o{}^2 r_o/Eh)]^{1/2}} \tag{20}$$

Large Bubbles and Cavitation Zones

At elbows or bends in the feedline, or at the pump inlet, local pressure drops are likely to create regions of cavitation. In most cases, these regions are composed of localized bubbles of vapor. These larger cavitation bubbles in the line are modeled by considering the bubbles to be local compliances. As the excitation frequency approaches the bubble resonant frequency, which can be quite low for large bubbles, the volume pulsations may be described by the following linear, second-order differential equation, assuming no phase changes occur:

$$\frac{\rho_l}{4\pi R_o}\ddot{v} + b\dot{v} + \frac{\eta P_o}{V_o}v = -p(t) \tag{21}$$

or, more simply

$$m_e\ddot{v} + b\dot{v} + v/C = -p(t) \tag{22}$$

The continuity equation relating the flow perturbations upstream and downstream of the bubble is

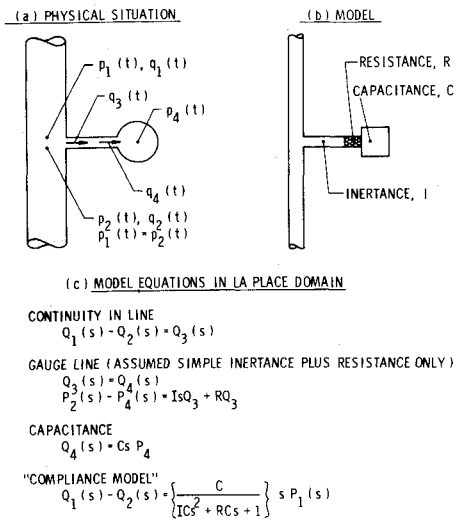

Fig. 5 Example treatment of more general "local compliance" in feed line.

$$q_2 - q_1 = dv/dt \tag{23}$$

Equations (22) and (23) can be combined conveniently in the Laplace domain to yield an expression for the change in flow rate due to the presence of the bubble.

$$Q_2(s) - Q_1(s) = -sP(s)/(m_e s^2 + bs + 1/C) \tag{24}$$

where the term $1/(m_e s^2 + bs + 1/C)$ can be visualized as a "complex" compliance. The damping term, b, has been estimated by Devin,[23] and is represented by a combination of thermal damping, sound radiation damping, and viscous damping. The thermal damping results from the thermal conduction between the gas in the bubble and the surrounding liquid. Sound radiation damping occurs because of energy dispersed by radiating spherical sound waves when the bubble is excited into volume pulsations, and viscous damping is created by viscous forces at the liquid-gas interface. The total damping coefficient is given by

$$b = b_{\text{th}} + b_{\text{rad}} + b_{\text{vis}} \tag{25}$$

where

$$b_{\text{th}} = \left[\frac{\dfrac{\sinh(2\phi R_o) + \sin(2\phi R_o)}{\cosh(2\phi R_o) - \cos(2\phi R_o)} - \dfrac{1}{\phi R_o}}{\dfrac{2\phi R_o}{3(k-1)} + \dfrac{\sinh(2\phi R_o) - \sin(2\phi R_o)}{\cosh(2\phi R_o) - \cos(2\phi R_o)}} \right] \times \frac{\eta P_o}{V_o \omega} \tag{26}$$

$$b_{\text{rad}} = \rho_l \omega^2 / 4\pi c_l \tag{27}$$

$$b_{\text{vis}} = \mu / \pi R_o^3 \tag{28}$$

Also, the argument

$$\phi R_o = (\omega/2D)^{1/2} R_o \tag{29}$$

is a measure of the rate at which heat is conducted over a distance, R_o, from the bubble center to the liquid-gas interface.

For a bubble undergoing successive compressions, the gas near the center behaves adiabatically, while the gas near the liquid-gas interface undergoes no change in temperature since the liquid behaves as a large heat sink. The correct value of the polytropic exponent, η, depends on the bubble size and excitation frequency. The value of the polytropic exponent has been found to be

$$\eta = \frac{k[1 + \delta_{\text{th}}^2]^{-1}}{\left[1 + \dfrac{3(k-1)}{2\phi R_o}\left(\dfrac{\sinh(2\phi R_o) - \sin(2\phi R_o)}{\cosh(2\phi R_o) - \cos(2\phi R_o)}\right)\right]} \tag{30}$$

where δ_{th} is equal to the term in brackets in Eq. (26).

Complex Side Branch

In general, any type of complicated side element, such as a gauge and line connected to a feedline, may be modeled. These side elements can be visualized as local or lumped "compliances," even though they may not be truly compliance-like in character. The model used for an arbitrary complex side element may be put in the form of a local compliance, as shown in Fig. 5. This element is assumed to consist of a side branch line having an inertance, I, and resistance, R, and with a capacitance termination, C. The line inertance and resistance have been programmed, respectively, as

$$I = \rho_o L/A \tag{31}$$

and

$$R = 8\mu L/\pi r_o^4 \tag{32}$$

To consider the effects of compressibility in the side branch, the inertia and resistance effects are neglected, and

$$q_4 = C\frac{dp}{dt}; \quad C = \frac{V_o}{kP_o} \text{ for gases} \qquad C = \frac{V_o}{\kappa} \text{ for liquids} \tag{33}$$

where q_4 is the flow into the branch.

When a gauge is connected to the propellant filled feedline by a branch line that is partially filled with air, the lumped model is obtained by summing the effects of the branch inertance, resistance, and capacitance.

The resultant expressions in the Laplace domain relating the pressure and flow upstream and downstream of the side branch become

$$P_2(s) = P_1(s) \tag{34a}$$

$$Q_2(s) = Q_1(s) - \left[\frac{C}{ICs^2 + RCs + 1}\right] sP_1(s) \tag{34b}$$

The quantity in the brackets can be visualized as a complex "compliance." For this case, it represents a local compliance insofar as the feedline is concerned.

Bellows

Bellows are commonly used elements in propulsion feed systems, and, in some applications,[24] they serve as a "fix" for the POGO instability. Bellows vary in their structural complexity from the simple array of axisymmetric convolutes shown in Fig. 6a to the configuration in Fig. 6b which incorporates a liner.

When the ends of a bellows experience relative motion, the change in volume flow rate between inlet and exit may be assumed to consist of the sum of 1) the flow rate change due to the compliance of the trapped gas, and 2) an apparent local volume production. The perturbation pressure drop across a bellows in the flow direction depends on the loss factor, f, which is dependent on the dynamic pressure and bellows geometry.

$$P_2(s) = fP_1(s) \tag{35}$$

The perturbation flow rate upstream and downstream of a gas volume are related in the physical domain by

$$q_2' - q_1' = -C(dp_1/dt). \tag{36}$$

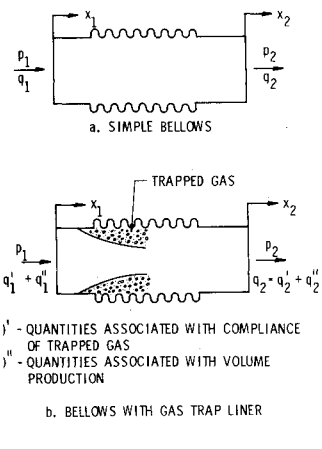

Fig. 6 Nomenclature for relative motion of bellows.

The apparent volume production was derived from the perturbation continuity equation

$$q_2'' - q_1'' = dv/dt \tag{37}$$

Summing the two effects in the Laplace domain

$$Q_2 - Q_1 = -CsP_1(s) + sV(s) \tag{38}$$

The volume production is related to the axial displacement of the bellows ends by

$$V(s) = k_b[X_1(s) - X_2(s)] \tag{39}$$

Equations (35) and (38) describe completely the four-terminal pressure-flow relationships for a bellows.

Forced Changes in Line Length

Propellant feedlines are normally supported by the vehicle structure at discrete points on the line as opposed to a continuous support. A forced change in the length of line between consecutive supports occurs when vehicle structural inputs to these supports differ in phase and/or magnitude. In an idealized fashion, it can be assumed that the length change is a result of discrete velocity inputs at the extremities of the line, as shown in Fig. 7.

Distributed forced changes in line length have been modeled, requiring the solution of the fluid dynamic equations of motion subject to an inhomogeneous boundary condition on the spatial variation of axial wall velocity as dictated by the structural inputs $\dot{x}_1$ and $\dot{x}_2$. The Laplace transform version of the linearized 1) radial and axial equations of motion for the fluid, 2) continuity equation, and 3) the equation of state for a fluid were reduced to one-dimensional form by averaging across the feedline cross section. The solution of the resultant differential equations for the transformed axial velocity was matched to the transformed, inhomogeneous, compatibility condition on wall velocity. This boundary condition was obtained by solving the undamped wave equation for the wall.[25] The resulting transformed pressure-flow perturbation equations are

$$\begin{bmatrix} P_2 \\ Q_2 \end{bmatrix} = \begin{bmatrix} \cosh \gamma L & -Z_c/A \sinh \gamma L \\ -Z_c^{-1} A \sinh \gamma L & \cosh \gamma L \end{bmatrix} \begin{bmatrix} P_1 \\ Q_1 \end{bmatrix} - \frac{\left(\frac{s^2}{c_o^2} - \gamma^2\right) U_w(s)}{\left(\frac{s^2}{c_w^2} - \gamma^2\right)} \begin{bmatrix} \alpha_1 \\ A\alpha_2 \end{bmatrix} \tag{40}$$

where

$$\alpha_1 = \frac{\rho_o c_o^2}{s} \left[\left(\frac{s}{c_w} \sinh \frac{sL}{c_w} - \gamma \sinh \gamma L \right) + \frac{\left(G - \cosh \frac{sL}{c_w}\right)}{\sinh \frac{sL}{c_w}} \frac{s}{c_w} \times \left(\cosh \frac{sL}{c_w} - \cosh \gamma L \right) \right]$$

$$\alpha_2 = -\left[\left(\cosh \frac{sL}{c_w} - \cosh \gamma L \right) + \frac{\left(G - \cosh \frac{sL}{c_w}\right)}{\sinh \frac{sL}{c_w}} \left(\sinh \frac{sL}{c_w} - \frac{s}{c_w \gamma} \sinh \gamma L \right) \right]$$

In these expressions c_w is the longitudinal wave speed in the wall and $G(s)$ is the transfer function relating the structural velocities, $\dot{x}_1$ and $\dot{x}_2$. It is evident that the effect of forced line changes is to modify the pressure-flow relationship for a line

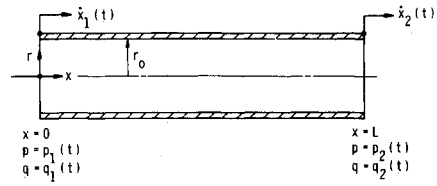

Fig. 7 Geometry for forced changes in line length.

with no external excitation. It can be shown that when $\dot{x}_1 = \dot{x}_2$, the above expressions degenerate to

$$\begin{bmatrix} P_2 \\ Q_2 \end{bmatrix} = \begin{bmatrix} \cosh \gamma L & -Z_c A^{-1} \sinh \gamma L \\ -AZ_c^{-1} \sinh \gamma L & \cosh \gamma L \end{bmatrix} \begin{bmatrix} P_1 \\ Q_1 \end{bmatrix} + U_w(s)\zeta \begin{bmatrix} Z_c \sinh \gamma L \\ A(1 - \cosh \gamma L) \end{bmatrix} \tag{41}$$

where $\zeta = 2J_1(\xi r_o)/\xi r_o J_o(\xi r_o)$, and $U_w(s)$ = transformed wall velocity. This latter result was predicted by Gerlach[22] for the rigid body, axial vibration of a line, where coupling occurs through viscous shear.

Mounting Stiffness

Propellant feedlines are anchored to the primary vehicle structure by mounting brackets that exhibit varying degrees of elasticity and damping. These brackets act as filters which modify the structural excitation that is transmitted to the feedline. This situation has been handled analytically by considering the idealized configuration shown in Fig. 8. The entire line, which has two bends, is assumed to be infinitely rigid and elastically restrained. A single linear spring in parallel with a viscous damper represents the combined effect of all the discrete mounting stiffnesses whose line of action coincides with that of the equivalent mounting stiffness. The resultant line acceleration, $a(s)$, has been determined in terms of the applied structural acceleration, $a_i(s)$, the viscoelastic support parameters and the fluid mass contained in the horizontal limbs of the feedline. During oscillatory motion, the mass of fluid contained in these horizontal limbs contributes an added mass, $(m_1 + m_3)$ effect. The inertial loading, caused by the fluid mass in the vertical segment of the line, has been replaced by its equivalent dynamic pressure forces on the projected areas of the elbows. Solution in the Laplace domain yields

$$a(s) = a_i(s)\left[\frac{sb + K}{Ms^2 + sb + K}\right] + A(P_3 - P_2)\left[\frac{s^2}{Ms^2 + sb + K}\right] \tag{42}$$

where M is the fluid mass of the oscillator. The resulting pressure-flow perturbation relation is

$$\begin{bmatrix} P_3 \\ Q_3 \end{bmatrix} = \begin{bmatrix} \frac{\cosh \gamma L + \beta'}{1 + \beta'} & \frac{-Z_c A^{-1} \sinh \gamma L}{1 + \beta'} \\ \frac{-Z_c^{-1} A \sinh \gamma L + \beta''(1 - \cosh \gamma L)}{1 + \beta'} & \frac{\cosh \gamma L + \beta'' Z_c A^{-1} \sinh \gamma L}{1 + \beta'} \end{bmatrix} \times \begin{bmatrix} P_2 \\ Q_2 \end{bmatrix} - \frac{a_i(s)}{1 + \beta'} \begin{bmatrix} \alpha' \\ \alpha'' \end{bmatrix} \tag{43}$$

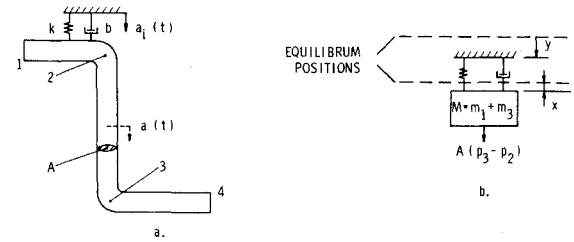

Fig. 8 Model for a line with mounting stiffness.

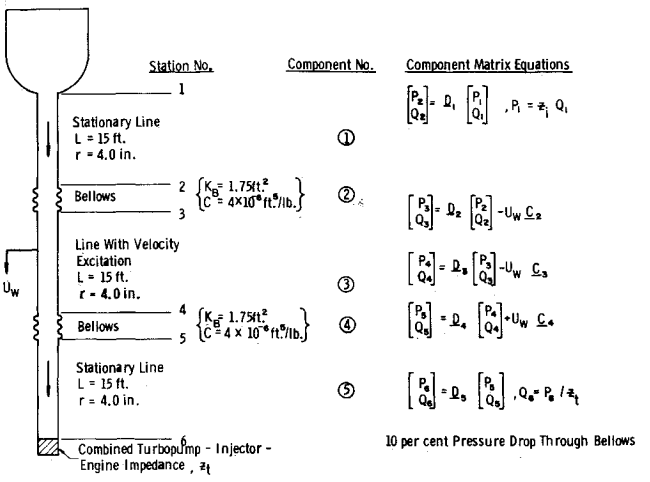

Fig. 9 Line model for example problem.

where

$$\alpha' = \frac{sb+K}{s(Ms^2+bs+K)} Z_c \sinh \gamma L$$

$$\beta' = \frac{As}{(Ms^2+bs+K)} Z_c \sinh \gamma L$$

$$\alpha'' = \frac{sb+K}{s(Ms^2+bs+K)} A(1-\cosh \gamma L)$$

and

$$\beta'' = \frac{A^2 s(1-\cos \gamma L)}{Ms^2+bs+K}$$

Generalized Computer Code

A versatile computer code was generated to calculate the frequency response of propellant feedlines. The program alleviates the time-consuming engineering task of reprogramming each different feedline design by providing the systems engineer with a design tool for obtaining the frequency response of a feedline in which the type, number, and sequence of basic line components between the propellant tank and the turbopump inlet can be specified in a completely arbitrary fashion. The dominant criterion employed in generating this code was that the user be required to perform a minimal amount of manual conditioning of a given problem prior to machine execution.

Formulation of the code was based on the four terminal matrix representation of the input-output pressure-flow relationship for a line component in the Laplace domain, e.g., Eqs. (8) and (41). The form of these equations can be generalized as follows:

$$\begin{bmatrix} P_{i+1} \\ Q_{i+1} \end{bmatrix} = \mathbf{D}_i \begin{bmatrix} P_i \\ Q_i \end{bmatrix} \pm F\mathbf{C}_i; \quad i = 1,2,\ldots,n \tag{44}$$

where n represents the number of components in the line. The transformed output pressure and flow for a given component are related to the corresponding input quantities through a 2×2 square matrix, $\mathbf{D}_i$, plus a column matrix, $\mathbf{C}_i$, that is present only if that particular component is being excited by an external forcing function, F. This scalar forcing function may be a structural velocity, acceleration or pulser flow perturbation. In general, it is desired to determine the perturbation pressure at some point in the line in response to any one of these forcing functions. With regard to propellant feedline analyses, the important pressure point is located at the turbopump inlet because dynamic variations in the inducer inlet suction head are instrumental in the growth of POGO type instabilities.

The functional form of the transfer equation for the over-all line is obtained by applying Eq. (44) to each line component, followed by manual matrix substitution to arrive at the generalized transfer equation

$$\mathbf{P} = \mathbf{DQ} \pm F\mathbf{B} \tag{45}$$

Matrix **P** in Eq. (45) contains the desired pressure response to the excitation, F, and matrix **Q** contains the pressure and flow perturbations at the exit to the fuel tank. The structure of matrix **D** can be stated a priori

$$\mathbf{D} = \mathbf{D}_n \mathbf{D}_{n-1} \mathbf{D}_{n-2} \cdots, \mathbf{D}_1 \tag{46}$$

Matrix **B**, however, does not possess such a well-defined property. In general,

$$\mathbf{B} = \mathbf{B}_1 + \mathbf{B}_2 + \cdots + \mathbf{B}_m \tag{47}$$

The value of "m" is strongly dependent on the line configuration as is the matrix structure of each $\mathbf{B}_j$. The distinguishing feature of each $\mathbf{B}_j$ is that it consists of a column matrix of one of the $\mathbf{C}_i$'s pre-multiplied by one or more $\mathbf{D}_i$'s. By assuming that the impedance at the tank exit, Z_i, is known and that the turbopump-injector-engine combination can be lumped into an equivalent terminal impedance Z_t, Eq. (45) can be expanded into its constituent equations to obtain the explicit form of the transfer function

$$\frac{P_n}{F} = \pm \frac{[(d_{21}Z_i + d_{22})b_{11} - (d_{11}Z_i + d_{12})b_{21}]}{(d_{21}Z_i + d_{22}) - (d_{11}Z_i + d_{12})/Z_t} \tag{48}$$

where b_{ij} and d_{ij} are the elements of the matrices, **B** and **D**, in Eq. (45).

The foregoing discussion forms the basis for constructing a computer code to determine the frequency response of a feedline containing an arbitrary number and sequence of components. The computer program, which was written in Fortran IV for a CDC 6400 computer, contains a controller program and a separate subroutine for each line component in which the elements of each $\mathbf{D}_i$ and $\mathbf{C}_i$ are calculated in the complex frequency domain. The program has the capability of synthesizing a feedline with as many as 11 different components. In addition, the source deck contains two subroutines with the appropriate logic for constructing matrices **B** and **D**. The Bessel functions, J_o and J_1, with complex arguments are evaluated using series expansions given by Watson.[26] The flow of subsequent calculations in the program is governed by the following inputs: 1) A coded set of integers describing the type of elements in the order in which they appear in the line, 2) the number of $\mathbf{B}_i$'s that are to be summed to arrive at matrix **B**, and 3) the number and type of matrices that are contained in each $\mathbf{B}_i$.

Using the codes in item (1), additional data, relevant to each component type, are read in and associated with a specific component location in the line. Reference 25 contains a user's manual and a complete print out of the general feedline computer code. Typical run times for most problems of practical interest are of the order of 20 sec.

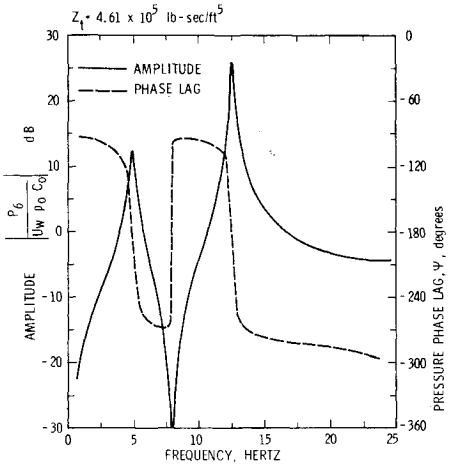

Fig. 10 Frequency response of example problem.

Example Problem

To illustrate the concepts that have been presented, consider the example shown in Fig. 9, which simulates a feedline containing LOX. The matrix equation for the terminal pressure response, P_6, due to the line excitation velocity, $U_w(s)$, is obtained by manually performing the previously indicated matrix substitutions.

$$\begin{bmatrix} P_6 \\ P_6/Z_t \end{bmatrix} = \mathbf{D}_5\mathbf{D}_4\mathbf{D}_3\mathbf{D}_2\mathbf{D}_1 \begin{bmatrix} Z_i Q_1 \\ Q_1 \end{bmatrix} + U_w(s)(\mathbf{D}_5\mathbf{C}_4 - \mathbf{D}_5\mathbf{D}_4\mathbf{C}_3 - \mathbf{D}_5\mathbf{D}_4\mathbf{D}_3\mathbf{C}_2) \quad (49)$$

Through the use of an appropriate set of control integers and physical properties of the fluid-filled line, Eq. (49) is converted, within the program, to the form of Eq. (48) and is evaluated at prescribed frequency points. The frequency response (amplitude and phase angle) of this configuration is shown in Fig. 10.

Conclusions

An analytical model and its corresponding computer program have been developed to generate the frequency response of an arbitrary liquid propellant feedline configuration. The model includes the effects of a viscous, turbulent mean flow, distributed wall compliances (elastic effects), entrained ullage gases or propellant vapor, local compliances, complex side branches, bellows, forced distributed changes in line length, and coupled structural accelerations with mounting stiffness. The computer program has been organized such that the amplitude and phase angle for the ratio of the terminal pressure to input excitation is calculated over any desired frequency range.

Investigation has shown that the predominant effect of turbulence is to increase the spatial attenuation at low frequencies; at high frequencies, the laminar and turbulent attenuations coincide. An additional factor, γ_t, has been added to the laminar propagation operator to account for the turbulent attenuation contribution. The reduction of phase velocity with turbulence can be neglected for all feedlines where $r_o^2\omega/\nu > 10^4$, which included virtually all cases of interest. The effect of wall compliance has been modeled by the classic Korteweg correction to the phase velocity, and the attenuation for the elastic wall has been found to be virtually indistinguishable from that for a rigid wall.

References

[1] Ryan, R. S., Kiefling, L. A., Jarvinen, W. A., and Buchanan, H. J., "Simulation of Saturn V S-II Stage Propellant Feedline Dynamics," *Journal of Spacecraft and Rockets*, Vol. 7, No. 12, Dec. 1970, pp. 1407–1412.

[2] Rubin, S., "Prevention of Coupled Structure-Propulsion Instability (POGO) on the Space Shuttle," Space Transportation System Technology Symposium, NASA TM X-52876, Vol. II, July 1970, pp. 249–262.

[3] Rubin, S., "Longitudinal Instability of Liquid Rockets Due to Propulsion Feedback (POGO)," *Journal of Spacecraft and Rockets*, Vol. 3, No. 8, Aug. 1966, pp. 1188–1195.

[4] "Investigation of 17-Hertz Closed-Loop Instability on S-II Stage of Saturn V," NASA Contract NAS8-19, Aug. 1969, Rocketdyne/NAR, Conoga Park, Calif.

[5] Sack, I. E. and Nottage, H. B., "System Oscillations Associated with Cavitating Inducers," *Journal of Basic Engineering*, Vol. 87, Series D, No. 4, Dec. 1965, pp. 917–924.

[6] Reardon, F. H., "Analytical Models of Low and Intermediate Frequency Instability," *Liquid Propellant Rocket Combustion Instability*, NASA SP-194, 1972, Chap. 5, pp. 233–263.

[7] Sabersky, R. H., "Effect of Wave Propagation in Feedlines on Low-Frequency Rocket Instability," *Jet Propulsion*, Vol. 24, No. 3, 1954, pp. 172–174.

[8] Woods, W. A., "Method of Calculating Liquid Flow Fluctuations in Rocket Motor Supply Pipes," *American Rocket Society Journal*, Vol. 31, No. 11, 1961, pp. 1560–1567.

[9] Wood, D. J., Dorsch, R. G., and Lightner, C., "Digital Distributed Parameter Model for Analysis of Unsteady Flow in Liquid-Filled Lines," TN-D-2812, 1965, NASA.

[10] Dorsch, R. G., Wood, D. J., and Lightner, C., "Distributed Parameter Analysis of Pressure and Flow Disturbances in Rocket Propellant Feed Systems," TN-D-3529, 1966, NASA.

[11] Fashbaugh, R. H. and Streeter, V. L., "Resonance in Liquid Rocket Engine Systems," *Transactions of the ASME, Journal of Basic Engineering*, Dec. 1965, Vol. 87, No. 4, pp. 1011–1018.

[12] Zielke, W., Wylie, E. B., and Keller, R. B., "Forced and Self-Excited Oscillations in Propellant Lines," *Transactions of the ASME, Journal of Basic Engineering*, Vol. 91, 1969, pp. 671–677.

[13] Rose, R. G., "Dynamic Analysis of Longitudinal Instability in Liquid Rockets," AIAA Paper 66-472, Los Angeles, Calif., 1966.

[14] Wing, H. and Tai, C. L., "A Study of Longitudinal Oscillations of Propellant Tanks and Wave Propagations in Feedlines," Rept. SID 66-46-1, Contract NAS8-11490, March 1966, North American Aviation, El Segundo, Calif.

[15] D'Souza, A. F. and Oldenberger, R., "Dynamic Response of Fluid Lines," *Transactions of the ASME, Series D: Journal of Basic Engineering*, Vol. 86, No. 3, Sept. 1964, pp. 589–598.

[16] Iberall, A. S., "Attenuation of Oscillatory Pressures in Instrument Lines," *Journal of Research*, National Bureau of Standards, Vol. 45, July 1950, pp. 85–106.

[17] Brown, F. T., "The Transient Response of Fluid Lines," *Transactions of the ASME, Series D: Journal of Basic Engineering*, Vol. 84, No. 4, Dec. 1962, pp. 547–553.

[18] Brown, F. T., Margolis, D. L., and Shah, R. P., "Small Amplitude Frequency Behavior of Fluid Lines with Turbulent Flow," *Transactions of the ASME, Journal of Basic Engineering*, Vol. 91, No. 4, Dec. 1969, pp. 678–693.

[19] Gouse, S. W. and Brown, G. A., "Survey of the Velocity of Sound in Two-Phase Mixtures," ASME Paper 64-WA/F3-35, New York, 1964.

[20] Hsieh, D.-Y. and Plesset, M. S., "On the Propagation of Sound in a Liquid Containing Gas Bubbles," *The Physics of Fluids*, Vol. 4, No. 3, Aug. 1969, pp. 970–975.

[21] Plesset, M. S. and Hsieh, D.-Y., "Theory of Gas Bubble Dynamics in Oscillating Pressure Fields," *The Physics of Fluids*, Vol. 3, No. 6, Dec. 1960, pp. 882–892.

[22] Gerlach, C. R., "The Dynamics of Viscous Fluid Transmission Lines with Particular Emphasis of Higher Mode Propagation," PhD thesis, July 1966, Oklahoma State University, Okla.

[23] Devin, C., Jr., "Survey of Thermal, Radiation, and Viscous Damping of Pulsating Air Bubble in Water," *Journal of the Acoustical Society of America*, Vol. 31, No. 72, Dec. 1959, pp. 1654–1667.

[24] Lewis, W. and Blade, R. J., "Analysis of Effect of Compensating-Bellows Device in a Propellant Line as a Means of Suppressing Rocket Pump Inlet Perturbations," TN D 2409, 1964, NASA.

[25] Holster, J. L., Astleford, W. J., and Gerlach, C. R., "Analysis of Propellant Feedline Dynamics," Final Rept. NAS8-25919, May 1973, Southwest Research Institute, San Antonio, Texas.

[26] Watson, G. N., *A Treatise on the Theory of Bessel Functions*, 2nd ed., Cambridge Press, 1952, Cambridge, Mass.